H3K4me3 plays a key role in establishing permissive chromatin states during bud dormancy and bud break in apple

Wenxing Chen[1,2], Yosuke Tamada[3,4,5], Hisayo Yamane[1,*], Miwako Matsushita[1], Yutaro Osako[6], Mei Gao-Takai[7], Zhengrong Luo[2], Ryutaro Tao[1]

[1]Graduate School of Agriculture, Kyoto University, Japan; [2]Key Laboratory of Horticultural Plant Biology, Huazhong Agricultural University, China; [3]School of Engineering, Utsunomiya University, Japan; [4]National Institute for Basic Biology, Japan; [5]The Graduate University for Advanced Studies, SOKENDAI, Japan; [6]Faculty of Agriculture, Shinshu University, Japan; [7]Agricultural Experimental Station, Ishikawa Prefectural University, Japan

Running title

The key role of H3K4me3 in bud dormancy regulation

Keywords: epigenome, histone methylation, H3K4me3, H3K27me3, apple (*Malus* × *domestica*), bud break, bud dormancy, *DORMANCY-ASSOCIATED MADS-box/SHORT VEGETATIVE PHASE* (*DAM/SVP*), *FLOWERING LOCUS C* (*FLC*), phytohormone

Corresponding author:

Hisayo Yamane

Graduate School of Agriculture, Kyoto University, Kyoto 606-8502, Japan

E-mail: yamane.hisayo.6n@kyoto-u.ac.jp

SUMMARY

Bud dormancy helps woody perennials survive winter and activate robust plant development in the spring. For apple (*Malus* × *domestica*), short-term chilling induces bud dormancy in autumn, then prolonged chilling leads to dormancy release and a shift to a quiescent state in winter, with subsequent warm periods promoting bud break in spring. Epigenetic regulation contributes to seasonal responses such as vernalization. However, how histone modifications integrate seasonal cues and internal signals during bud dormancy in woody perennials remains largely unknown. Here, we show that H3K4me3 plays a key role in establishing permissive chromatin states during bud dormancy and bud break in apple. The global changes in gene expression strongly correlated with changes in H3K4me3, but not H3K27me3. High expression of *DORMANCY-ASSOCIATED MADS-box* (*DAM*) genes, key regulators of dormancy, in autumn was associated with high H3K4me3 levels. In addition, known DAM/SHORT VEGETATIVE PHASE (SVP) target genes significantly overlapped with H3K4me3-modified genes as bud dormancy progressed. These data suggest that H3K4me3 contributes to the central dormancy circuit, consisting of DAM/SVP and abscisic acid (ABA), in autumn. In winter, the lower expression and H3K4me3 levels at *DAM*s and gibberellin metabolism genes control chilling-induced release of dormancy. Warming conditions in spring facilitate the expression of genes related to phytohormones, the cell cycle, and cell wall modification by increasing H3K4me3 toward bud break. Our study also revealed that activation of auxin and repression of ABA sensitivity in spring are conditioned at least partly through temperature-mediated epigenetic regulation in winter.

INTRODUCTION

Bud dormancy, during which the bud is unable to resume growth, is an important adaptive trait for the survival and growth of perennial plants native to temperate and boreal regions (Cooke *et al.*, 2012). In apple (*Malus* × *domestica*), which is an economically important fruit tree species in the Rosaceae family, bud dormancy is induced in response to short-term low temperatures in autumn regardless of the photoperiod (Heide and Prestrud, 2005). Exposure to a specific and genetically determined chilling period, known as chilling requirement fulfillment, ensures that buds are released from dormancy (mainly referred to as endodormancy). During this dormancy release period, bud growth remains repressed due to the limited availability of growth-promoting factors in winter, such as warm conditions, water, and nutrients. This state is known as the quiescent state (or ecodormancy) (Lang *et al*., 1987; Considine and Considine, 2016). Exposure to a subsequent warming period, known as heat requirement (HR) fulfillment, allows buds to be released from quiescence, thereby enabling bud break and normal blooming in spring.

Bud dormancy pathways in woody perennial species form complex interconnections involving responses to oxidative stress and reactive oxygen species, phytohormone biosynthesis and signaling pathways, cell wall loosening, cell cycle reentry, and lipid metabolism (Azeez *et al*., 2021; Saito *et al.*, 2017; Beauvieux *et al.*, 2018). The abscisic acid (ABA), gibberellic acid (GA), and auxin pathways are critical for regulating bud dormancy establishment, release, and bud break (Liu and Sherif, 2019). ABA plays a central role in bud dormancy in woody perennials (Tylewicz *et al*., 2018; Zheng *et al*., 2018) and closes the plasmodesmata of dormant buds in the apical meristem of hybrid aspen (*Populus tremula* × *tremuloides*) trees (Tylewicz *et al*., 2018). ABA and GAs have antagonistic roles: A prolonged exposure to chilling temperatures induces dormancy release together with a decrease in ABA levels in buds (Tylewicz *et al*., 2018), while also promoting the expression of GA biosynthesis and signaling genes in hybrid aspen (Rinne *et al*., 2011). In addition, transcriptome profiling of apple dormant buds revealed that auxin biosynthesis and transport are involved in the

regulation of dormancy progression (Porto *et al*., 2015; Takeuchi *et al*., 2018).

In fruit trees from the Rosaceae family, *DORMANCY-ASSOCIATED MADS-box* (*DAM*) genes encoding members of the SHORT VEGETATIVE PHASE (SVP)/AGAMOUS-LIKE24 (AGL24) clade of MADS-box transcription factors are thought to play a key role in bud dormancy (Falavigna *et al.*, 2019; Hsiang *et al.*, 2021; Wu *et al.*, 2021). Expression of *DAM*s is induced by short-term chilling in buds to establish the dormant state, only to be repressed by prolonged exposure to chilling for dormancy release (Sasaki *et al*., 2011; Leida *et al.*, 2012; Falavigna *et al*., 2021). Rosaceae *DAM*s promote ABA biosynthesis (Tuan *et al*., 2017), accumulation in buds (Yamane *et al*., 2019), and signaling (Falavigna *et al*., 2021). Moreover, ABA enhances the transcription of *DAM3* in Japanese pear (*Pyrus pyrifolia*) (Yang *et al*., 2020). These data suggest the existence of a positive feedback circuit involving ABA and *DAM* genes to establish the dormancy state in autumn. In apple, MdDAM forms a protein complex with MdSVPa to control the dormancy cycle (Falavigna *et al*., 2021).

The release of bud dormancy is thought to involve epigenetic changes in gene expression through histone modifications (Ríos *et al*., 2014; Conde *et al*., 2019), by analogy with vernalization (Michaels and Amasino, 1999). Both processes are induced by prolonged exposure to cold temperatures, the memory of which remains even after plants are returned to warmer conditions (Horvath, 2009; Brunner *et al*., 2014). In plants, lysine modifications on histone H3 tails, such as lysine 4 trimethylation (H3K4me3) and lysine 27 trimethylation (H3K27me3), are currently considered to be the main contributors of epigenetic regulation during plant development (Xiao *et al.*, 2016). H3K4me3 is a euchromatin mark mainly distributed around the transcription start site of actively transcribed genes (Zhang *et al.*, 2009; Zhang *et al.*, 2016). By contrast, H3K27me3 is enriched across the transcribed regions of genes that are usually transcriptionally inactive and exhibit tissue specificity (Zhang *et al.*, 2007).

In Brassicaceae species, the MADS-box transcription factor FLOWERING LOCUS C (FLC) represses flowering until the plant is exposed to the extended cold of winter during the vernalization response. Prolonged chilling results in higher H3K27me3 and lower H3K4me3 levels at the *FLC* locus to stably repress *FLC*

transcription even after plants are returned to warmer temperatures (Bastow *et al*., 2004; Sung *et al*., 2004; Tamada *et al*., 2009). Notably, the role and expression pattern of *FLC* orthologs in apple are different from their Brassicaceae counterparts. In apple, prolonged chilling induces the high expression of an *FLC-like* gene that is supposed to repress bud break during the quiescent stage in winter (Falavigna *et al*., 2021; Hsiang *et al*., 2021; Nishiyama *et al*., 2021). In this regard, *DAM* genes exhibit a molecular behavior closer to that of *FLC*; the repression of *DAM* expression caused by prolonged chilling is associated with increased H3K27me3 levels at *DAM* loci (de la Fuente *et al*., 2015; Vimont *et al*., 2020; Zhu *et al*., 2020). However, the possible involvement of histone modifications in other critical pathways, including phytohormone signaling, during apple bud dormancy and break remains unknown.

In this study, we generated global epigenome and transcriptome profiles of dormant apple buds at three critical stages during bud dormancy and break, namely, before fulfillment of the chilling requirement in autumn (stage BC for before prolonged chilling), after fulfillment of the chilling requirement (5°C for 60 days) in winter (stage AC for after prolonged chilling), and during subsequent fulfillment of the heat requirement (22°C for 9 days) in early spring (stage BB for bud break). We determined that H3K4me3 marks exert a dominant role over H3K27me3 in temperature-mediated global changes of gene expression, including those related to phytohormone biosynthesis and signaling, the cell cycle, and cell wall modification pathways. We also explored the H3K4me3 and H3K27me3 modifications at the *DAM* and *FLC* loci and observed significant overlap between SVP/DAM/FLC target genes and H3K4me3-modified genes in apple buds. Importantly, we identified multiple genes whose H3K4me3 levels changed first in winter, followed by changes in gene expression during early spring, suggesting an epigenetic role for H3K4me3 in the expression of these genes after plants return to warmer conditions. The data presented here thus provide novel insights into genome-wide histone methylation states during bud dormancy and break in apple.

RESULTS

H3K27me3/H3K4me3 marks in response to prolonged chilling and subsequent warm temperature

To examine changes in histone methylation during bud dormancy and bud break, we performed chromatin immunoprecipitation followed by deep sequencing (ChIP-seq) and transcriptome deep sequencing (RNA-seq) analyses using terminal apple buds at three critical stages, which were morphologically comparable with a moderate developmental progression of the flower meristem from BC to AC stages and no differences from AC to BB stages (Figures 1a and S1). This experimental setup therefore focused on the differences in epigenome and transcriptome between samples at distinct bud dormancy stages that are independent from possible secondary effects caused by morphological differences. ChIP-seq signals were robust among replicates and showed that H3K27me3 and H3K4me3 were enriched in the transcribed regions and around transcription start sites (TSSs) (Figure 1b,c), respectively, in agreement with results from multiple studies in other angiosperms (Zhang *et al.*, 2007; Zhang *et al.*, 2009).

To examine the significance of the resulting ChIP-seq signals, we conducted an unsupervised k-means clustering (k = 5) analysis using the ChIP-seq signals around genic regions (2-kb upstream from the TSS to 2-kb downstream from the transcription end site [TES] for H3K27me3 and 2-kb on either side of the TSS for H3K4me3). The genes from the top two clusters (1 and 2) with the highest H3K27me3 levels (Figure 1b) exhibited lower expression levels for all three stages relative to all other genes (Figure 1d). Conversely, genes from the top two clusters with the highest H3K4me3 levels had higher expression levels than all other genes (Figure 1c-d). These results supported the roles of H3K27me3 and H3K4me3 for repression and activation of gene expression in apple, which was consistent with other annual model plants like Arabidopsis (*Arabidopsis thaliana*) and rice (*Oryza sativa*) (Zhang *et al.*, 2007; Zhang *et al.*, 2009; Zhang *et al*., 2016).

Importantly, the signal density obtained for the input and total histone H3 samples was similar across all clusters and showed no differences between H3K27me3 and H3K4me3 controls (Figure S2), highlighting the specificity of the specific H3K27me3

and H3K4me3 signals. We also validated the specificity of the two antibodies used here by dot blot analysis using a modified histone peptide array (Figure S3).

Identification of potential contributors to histone modifications in apple buds

Histone modifications around TSSs, which strongly affect transcription, can be predicted from transcription factor (TF) binding at promoter regions and other regulatory regions in human cell lines, suggesting that certain TFs may have direct and indirect effects on histone modifications (Benveniste *et al*., 2014). To identify potential TF contributors to H3K27me3 or H3K4me3 in apple buds, we scanned for TF recognition motifs within the 2-kb promoter regions of genes enriched in H3K27me3 or H3K4me3 (clusters 1 and 2 in Figure 1b,c) using HOMER (Heinz *et al*., 2010). These scans identified multiple significantly overrepresented TF target motifs upstream of H3K27me3-enriched genes (Table S1), including binding sites for FUSCA3 (FUS3), LATERAL ORGAN BOUNDARIES (LOB)/ASYMMETRIC LEAVES2 (AS2), and APETALA2/ETHYLENE RESPONSIVE FACTOR (AP2/ERF) TFs.

Previous studies have reported that homologs of these TFs function in H3K27me3 methylation or demethylation in other land plants. FUS3 is a member of the B3 transcription factor ABA-INSENSITIVE3 (ABI3)/VIVIPAROUS-1 (Vp-1) family of TFs and mediates the deposition of different histone modifications at the *phaseolin* locus in the absence or presence of ABA (Ng and Hall, 2008). Recent work showed that ABI3 recruits a scaffold protein with active chromatin modifiers to reset *FLC* chromatin into an active state in late embryogenesis through the removal of H3K27me3 (Xu *et al*., 2022). The plant-specific LOB family of TFs comprises key regulators of plant organ development (Xu *et al.*, 2016). In Arabidopsis, the LOB domain protein AS2 recruits the Polycomb repressive complex at *KNOTTED1-LIKE HOMEOBOX* (*KNOX*) loci to repress their transcription via H3K27me3 deposition (Li *et al.*, 2016). The AP2/ERF factors influence plant hormone signal transduction, plant responses to environmental stresses (Dietz *et al.*, 2010), and bud break (Tuan *et al.*, 2016; Azeez *et al*., 2021). Moreover, AP2/ERF factors also affect plant regeneration by removing H3K27me3 modifications at stem cell identity genes (Ishikawa *et al.*, 2019).

Here, we identified GAGA factor BARLEY B RECOMBINANT (BBR)/BASIC PENTACYSTEINE (BPC)-targeting motifs, which were significantly overrepresented in the promoters of H3K4me3-enriched genes (Table S2). GAGA factors were first identified as Trithorax-group proteins that counteract the transcriptional repression imposed by Polycomb-group proteins and H3K27me3 modification, and activate transcription through histone modifications such as H3K4me3 (Berger and Dubreucq, 2012). These data suggest the potential importance of the above factors in transcriptional regulation through histone modifications in apple buds.

In addition, we found that SVP-targeting motifs were significantly overrepresented in the promoters of H3K4me3-enriched genes (Table S2). Rosaceae DAM proteins, key dormancy regulators, are thought to have diverged from SVP/AGL24-type MADS-box TFs (Figure S4a), and the apple SVP ortholog SVPa forms a protein complex with DAMs to control dormancy (Falavigna *et al*., 2021). To extend our understanding of the possible role of SVP/DAMs in regulating H3K4me3, we analyzed the overlap between SVP/DAM/FLC-target genes and H3K4me3-enriched genes (clusters 1 and 2 in at least one stage) in apple buds. Falavigna *et al.* (2021) identified 1,254, 718, 865, and 539 genes as high-confidence targets of the DAM1-SVP, DAM4-SVP, FLC-SVP, and SVP-SVP complexes in apple buds, respectively. Of these genes, 405, 258, 274, and 163 genes were enriched in H3K4me3 (Table S3) and were all significantly different from non-H3K4me3 genes (hypergeometric *P* values = $3.88e^{-44}$, $6.94e^{-37}$, $1.24e^{-28}$, and $1.53e^{-15}$, respectively). Given the indirect role of TFs in histone modifications (Benveniste *et al*., 2014), we hypothesized that DAM and SVP might indirectly contribute to H3K4me3 in apple buds, although functional analysis involving transformation is necessary to test this hypothesis.

The expression pattern of specific MADS-box genes involved in bud dormancy progression and break is associated with histone modifications

In light of the association between H3K4me3 and H3K27me3 levels and *DAM* gene expression during peach dormancy release (Leida *et al*., 2012; Vimont *et al*., 2020; Zhu *et al*., 2020) and *FLC* in Brassicaceae vernalization (Sung and Amasino, 2004; Tamada

et al., 2009), we investigated the H3K27me3 and H3K4me3 marks at apple *DAM* and *FLC* clade loci. Based on phylogenetic analysis, MADS-box TFs encoded by the current apple reference genome formed two groups: one containing four DAM members (DAM1, DAM2, DAM4, and DAMb) (Falavigna *et al*., 2021) and the other containing seven FLC-like proteins (Figure S4a). Among the seven FLC clade proteins, FLC1 to FLC4 have been reported previously (Zong *et al*. 2019; Hsiang *et al*. 2021). We confirmed the quality of the ChIP-seq datasets assembled in this study by checking the signals at *ELONGATION FACTOR1* (*EF1*) and *AGAMOUS* (*AG*), which are known to be enriched in H3K4me3 and H3K27me3 marks, respectively (Saito *et al*., 2015; Vimont *et al*., 2020). We detected high H3K4me3 or H3K27me3 signals at *EF1* and *AG*, respectively, across all stages (Figure S4b), thus validating our ChIP-seq data.

All four *DAM* genes exhibited lower expression from the BC to the AC stage (Figure 2a), which was accompanied by significantly ($P < 0.05$) decreased ABA contents (Figure 2b), indicating that the DAM-ABA circuit underlies the dormancy state also in our laboratory conditions. This decrease in *DAM* gene expression was associated with lower H3K4me3 levels at all four loci from the BC to the AC stage (Figure 2a; Table S4) and with higher H3K27me3 levels at *DAM1* (limited to around the TSS) and *DAM4* loci (over the entire gene body). These results suggest that decreased expression of *DAM1* and *DAM4* during dormancy release is regulated by both H3K4me3 and H3K27me3, while that of *DAM2* and *DAM3* is regulated by H3K4me3 only.

Three out of the seven *FLC* clade genes were not expressed at any of the three stages and were thus excluded from further analysis. Of the remaining four *FLC* clade genes (*FLC1*, *FLC2*/*FLC-like*, *FLC3*, and *FLC4*), *FLC1* and *FLC3* showed declining expression levels from the BC to the BB stage, while *FLC2* and *FLC4* reached their highest expression levels at the AC stage. The expression levels of *FLC2* were positively and negatively correlated with the pattern of H3K4me3 and H3K27me3 levels, respectively (Figure 2a; Table S4), suggesting that the transcription of *FLC2*, a key factor of the quiescent state, is regulated by these modifications. In addition, we observed that many RNA-seq reads map to intronic regions for all *FLC* loci, suggesting

the existence of non-coding RNAs similar to Arabidopsis *COOLAIR* and *COLDAIR*, which modulate the epigenetic silencing of *FLC*, and to kiwifruit long non-coding RNAs, which regulate chromatin state at an *FLC*-like gene (Swiezewski *et al*., 2009; Heo and Sung, 2011; Voogd *et al*., 2021). We detected the highest levels of H3K27me3 modification at the *DAM2*, *DAM4*, *DAMb*, *FLC3*, and *FLC4* loci at the BB stage, likely to maintain their repressed transcriptional state, as with Arabidopsis *FLC* (Buzas *et al*., 2011, 2012). The expression pattern of two *SVP-like* genes, *SVPa* and *SVPb*, was not associated with changes of histone modifications (Figure S4b). These results suggest that histone modifications are involved in the transcriptional regulation of several *DAM* and *FLC* genes during bud dormancy and break.

Changes in H3K4me3, but not H3K27me3, levels are associated with changes in gene expression during bud dormancy progression and break

We identified 2,953 and 11,723 differently modified genes (DMGs) by H3K27me3 and H3K4me3, respectively, between the three stages examined (comparing BC and AC, and AC and BB). We wished to analyze the effects of seasonal changes in H3K27me3 and H3K4me3 modification on gene expression. Of the above DMGs, we excluded 852 H3K27me3 DMGs and 2,549 H3K4me3 DMGs from further analysis based on their overall low expression levels (below 0.5 fragments per kilobase of transcript per million mapped reads [FPKM] across all stages). Of the remaining 2,101 H3K27me3 DMGs and 9,174 H3K4me3 DMGs, 506 DMGs were modified by both histone marks, suggesting a bivalent histone modification or a univalent histone modification acting in different sets of cells. The expression levels of H3K4me3 DMGs showed a high correlation with changes in H3K4me3 levels, but those of H3K27me3 DMGs displayed little correlation with H3K27me3 levels (Figure 3a). We thus decided to focus on the role of H3K4me3 on global gene expression during bud dormancy progression and break in this study. We will however acknowledge that the 1,114 H3K27me3 DMGs whose expression was negatively correlated with H3K27me3 levels may include key genes required for the regulation of bud dormancy and break (Table S5).

Since H3K4me3 levels showed a strong correlation with gene expression,

including that of the major regulators of dormancy *DAM*s, we analyzed which H3K4me3 patterns were overrepresented during bud dormancy and break by applying k-means clustering. Accordingly, we classified 7,050 H3K4me3 DMGs whose expression levels were positively correlated with H3K4me3 levels into four clusters (Figures 3b, S5a) (see Experimental Procedures). We confirmed the strong correlation between H3K4me3 and gene expression levels for each cluster, as evidenced by the similar heatmaps for each dataset (Figure 3b). Cluster 1 contained 1,859 genes, which were marked by H3K4me3 in both BC and AC stages or in the BC stage alone, including *SNF1-related protein kinase 2.7* (*SnRK2.7*), encoding a central regulator of ABA signaling (Figure 3c). Cluster 2 consisted of 642 genes, with strong H3K4me3 marks only in the AC stage, such as *C-terminal cysteine residue is changed to a serine family protein 1* (*CXXS1*). Cluster 3 comprised the largest number (3,911) of genes, with H3K4me3 marks only in the BB stage, including the *D-type cyclin* gene *CYCD3-2*. Cluster 4 contained 638 genes, which appeared to experience a loss of a H3K4me3 mark in the AC stage, essentially presenting a pattern opposite to that of cluster 2. The *GLIP* gene, encoding a GDSL-like lipase/acylhydrolase superfamily protein, was included in cluster 4.

We subjected each cluster to Gene Ontology (GO) analysis, which returned enrichment for terms associated with lipid metabolism for cluster 1 and with cell redox homeostasis for cluster 2, both of which are key metabolic pathways involved in dormancy regulation (Or *et al*., 2000; Saito *et al*., 2017) (Figure S5b). Notably, genes from the largest cluster, cluster 3, showed enrichment for GO terms involved in responses to phytohormones, regulation of cell cycle, and the plant-type cell wall organization–related pathway (Figure 3b; Table S6). Given that cell cycle reentry and cell wall loosening are necessary for bud break, we explored H3K4me3 and expression levels of differentially expressed genes (DEGs) with a role in these two processes between the three stages examined here (Figure 3d). We established that all 24 *CYC* DEGs (out of 45 *CYC* genes in the apple genome) exhibited the highest expression during the BB stage, which was mostly consistent with the highest H3K4me3 levels observed at this stage. In addition, a large fraction of DEGs associated with cell wall

loosening showed the highest expression at the BB stage relative to the other two stages: 26 out of 54 *expansin* (*EXPA/B*), 14 out of 38 *xyloglucan endotransglucosylase/hydrolase* (*XTH*), 13 out of 32 *pectate lyase* (*PL*), and 17 out of 88 cellulose metabolism–related *β-glucosidase* (*BGLU*) DEGs. Importantly, these genes also exhibited heavy H3K4me3 marks at the BB stage (Figure 3d). These results suggest that H3K4me3 plays a crucial role in global changes of gene expression related to cell cycle reentry and cell wall loosening during bud break.

H3K4me3 modifications at auxin- and GA-related genes during dormancy progression and toward bud break

As mentioned above, cluster 3 genes showed an enrichment for the GO term "response to phytohormones". Auxin and GA-related genes were included in this cluster, which was consistent with the role of auxin and GA in bud break. This observation prompted us to further explore the expression and H3K4me3 levels of DEGs involved in auxin and GA biosynthesis, metabolism, and signaling between the three stages.

Of 18 *YUCCA* (*YUC*) genes encoding key auxin biosynthesis enzymes (Zhao *et al*., 2001) in the apple genome, six were differentially expressed at the BB stage and were heavily marked with H3K4me3 (Figure 4). Similarly, among seven DEGs out of the 26 *PIN-FORMED* (*PIN*) genes encoding auxin efflux carriers, six genes exhibited high expression levels at the BB stage and with matching high H3K4me3 levels (Figure 4). Strikingly, 42 out of 98 *small auxin-up RNA* (*SAUR*), 10 out of 17 *GRETCHEN HAGEN3* (*GH3*), and six out of 31 *auxin/indole-3-acetic acid* (*Aux/IAA*) were differentially expressed with generally strong expression at the BB stage and displayed the highest H3K4me3 levels at this stage relative to the BC and AC stages (Figure 4). These results suggest that H3K4me3 underpins enhanced auxin reactions at the BB stage, especially acid growth mediated by SAURs (Stortenbeker and Bemer, 2019). For genes involved in GA biosynthesis and metabolism, one *GA 20-oxidase* (*GA20ox*) and two *3-oxidase* (*GA3ox*) were differentially expressed with high expression in the AC (*GA20ox*) or BB (*GA3ox*) stage, while four *GA2 oxidase* (*GA2ox*) genes encoding GA catabolic enzymes were differentially expressed with higher expression at the BC stage

compared to the AC or BB stage, with corresponding high H3K4me3 levels (Figure 4). These results indicate that GA precursors synthesized by GA20ox in winter promote the biosynthesis of active GAs by GA3ox in spring and that active GAs are vigorously catabolized to inactive GAs by GA2ox in autumn. In addition, among 15 DEGs out of 29 *gibberellic acid-stimulated Arabidopsis family* (*GASA*) genes, 13 DEGs exhibited the highest expression and H3K4me3 levels at the BB stage, indicative of active GA responses at this stage. The changes in expression described for the GA-related genes listed above were accompanied by changes in H3K4me3 levels and were consistent with the reported role for GAs in dormancy regulation.

Prolonged chilling–induced H3K4me3 changes have a causal role in the expression regulation of a set of genes toward warming-promoted bud break

We wished to identify genes whose expression levels showed signs of long-term environmental epigenetic memory. Such genes would be defined as exhibiting changes in histone modification levels at the AC stage (corresponding to winter), followed by later changes in their expression levels at the BB stage (equivalent to early spring) driven by epigenetic marks at each candidate locus. Based on the above criteria, we identified 76 (cluster 1) and 16 (cluster 2) genes whose H3K4me3 levels increased or decreased during the AC stage, with a later increase (cluster 1) or decrease (cluster 2) in their expression levels at the BB stage (Figure 5a,b). We considered these genes to be in a "ready to go/stop" state, as their histone methylation profile in the AC stage would dictate their transcriptional activation or repression during the warm conditions of the BB stage. Notably, we noticed the presence of genes related to auxin signaling and response in cluster 1, including three *SAUR* and three *AUXIN/INDOLE-3-ACETIC ACID* (*AUX/IAA*) genes (Figure 5a,c), as well as several genes encoding TFs (Table S7). The 16 genes in cluster 2 included the ABA receptor gene *PYRABACTIN-LIKE12* (*PYL12*)-*like* and *MYB30*, a homolog of *AtMYB15* involved in ABA and drought responses (Ding *et al*., 2009) (Figure 5a,c; Table S7).

We also identified 199 genes whose expression levels dropped from high levels at the BC stage to low levels during the AC stage, although their H3K4me3 levels

decreased later during the BB stage (cluster 3; Figure 5a; Table S7). We envisage that H3K4me3 depletion in spring likely reinforces the transcriptionally repressed state established during the previous winter. Among these genes, we identified 11 genes associated with ABA signaling and response, such as *ABA-RESPONSIVE ELEMENT BINDING FACTOR4* (*ABF4*), *ABA REPRESSOR1* (*ABR1*), and *ABA-INSENSITIVE2* (*ABI2*) (Figure 5a,c; Table S7). These results indicate that warming-induced reduction of H3K4me3 plays a reinforcing role to prevent the reactivation of gene expression for the ABA signaling pathways in the warmer conditions of spring. On the other hand, none of the genes exhibited increased expression at the AC stage followed by increased H3K4me3 levels at the BB stage.

DISCUSSION

Previous studies on the analysis of histone modifications during active growth and dormancy in perennial trees have largely focused on specific dormancy regulators, such as certain *DAM* genes in Rosaceae. Here, we incorporated epigenome data for H3K27me3 and H3K4me3, two key histone modifications involved in plant development, with deep transcriptome data across three key stages during dormancy progression and bud break to build a stage-by-stage map of histone marks linked to changes in gene expression.

The number of H3K4me3 DMGs was greater than that for H3K27me3 DMGs (Figure 3a). In addition, H3K4me3 DMGs showed a positive correlation between their changes in H3K4me3 and expression levels, while only some H3K27me3 DMGs exhibited a negative correlation between their H3K27me3 changes and expression levels. These results suggested that the H3K4me3 marks prevails over H3K27me3 in the regulation of global gene expression underlying the progression and break of apple bud dormancy. Nevertheless, H3K27me3 likely participates in the transcriptional regulation of key dormancy-related genes as well, including *DAM*s (Figure 2a; Table S4), as observed at the *FLC* locus during vernalization in Brassicaceae (Sung and Amasino, 2004).

In late autumn, the flower buds of temperate or boreal fruit tree species enter a dormant state, during which ABA and *SVP*/*DAM* orthologs are believed to form a positive feedback circuit and play key roles on growth inhibition and bud break repression (Falavigna *et al.*, 2019; Liu and Sherif, 2019; Yamane *et al.*, 2019; Yang *et al*., 2021). In this study, we showed that the expression of *DAM* genes is highest in the BC stage, which was associated with not only the highest ABA contents but also with the highest H3K4me3 levels (Figure 2). *DAM* expression levels then decreased, concomitantly with lower ABA contents and decreased H3K4me3 levels at all *DAM* loci and increased H3K27me3 levels at two *DAM* loci in winter. A correlation between changes in *DAM* expression and H3K4me3 and H3K27me3 levels was also observed in sweet cherry (*Prunus avium*) (Vimont *et al*., 2020), peach (Leida *et al.*, 2012; Vimont *et al*., 2020; Zhu *et al*., 2020), and leafy spurge (*Euphorbia esula*) (Horvath *et al.*, 2010). These data indicate that H3K4me3 and H3K27me3 modifications play a key role in the regulation of *DAM* gene expression during bud dormancy progression. In addition, we determined that the recognition motifs for SVP/DAM and another MADS-box protein (Mef2a) are enriched in the promoters of H3K4me3-modified genes (Table S2). In fact, the set of DAM-SVP and FLC-SVP target genes significantly overlapped with H3K4me3-enriched genes (Table S3), suggesting that SVP/DAM also contribute to the regulation of H3K4me3. Thus, we hypothesize that H3K4me3 participates in the SVP/DAM-ABA positive feedback circuit to ensure dormancy in late autumn (Figure 6; left part). We also propose that the regulation of histone methylation marks participates in the reduction of *DAM* expression and ABA contents (Figure 2) to control prolonged chilling-induced dormancy release in winter (Figure 6; center part). During the dormancy release period, buds remain in an inactive state due to the limited availability of growth-promoting factors in winter. *FLC2* is highly expressed during this stage and is considered to repress bud break (Falavigna *et al*., 2021; Nishiyama *et al*., 2021). In our study, prolonged chilling-induced *FLC2* expression at the AC stage and lower expression in the warmer conditions of the BB stage were positively and negatively correlated with changes in H3K4me3 and H3K27me3 marks, respectively (Figure 6; center part). We thus hypothesize that *FLC2* encoding a key quiescence factor

in winter is regulated by these histone methylations.

One of the striking effects of histone modifications is the activation of transcription by H3K4me3 at the BB stage (cluster 3 in Figure 3b). Indeed, over half of H3K4me3 DMGs (3,911 out of 7,050) were heavily marked with H3K4me3 at the BB stage and their transcription was induced; GO analysis revealed that these genes are mainly related to phytohormone response, cell cycle regulation, cell wall organization, photosynthesis, cytoskeleton organization, and microtube-related pathways. Multiple genes related to auxin biosynthesis, transport, and response were significantly up-regulated and reached their highest H3K4me3 levels at the BB stage (Figure 4). In addition, we observed the highest expression levels for *GA20ox* and *GA3ox* genes at the AC and BB stages, respectively, while the expression of *GA2ox* genes declined from the BC to the BB stage (Figure 4). These results reflect the low amount of active GAs in autumn, the rise in GA precursors in winter, and the high amount of active GAs in spring to promote bud break and growth, as reported in apple (Sapkota *et al.*, 2021) and Japanese apricot (Zhang *et al*., 2018). Accordingly, the GA signaling–related *GASA* genes were highly expressed in the BB stage. This observation was consistent with the previous report that the exogenous application of GA_4 promotes bud break in sweet cherry (Cai *et al*., 2019) and Japanese apricot (Zhuang *et al*., 2013), and GA biosynthesis increases toward bud break in Japanese apricot (Zhang *et al*., 2018). Together with the above genes, we determined that 24 *CYC* genes out of 45 were differentially expressed during our time course, reaching their highest expression levels when the H3K4me3 mark was most abundant at the BB stage (Figure 3d). Cell division increases when buds begin to grow outward in spring (Horvath *et al*., 2003), which relies on auxin signaling to affect both the transcriptional and posttranscriptional regulation of cell cycle components (Perrot-Rechenmann, 2010). The expression of genes related to the G1-to-S-phase transition, such as *CYCD*s and *cyclin-dependent kinase*s (*CDK*s), is one of the prerequisites for bud outgrowth (Shimizu-Sato and Mori, 2001; Aksenova *et al*., 2013). In addition, auxin was also reported to be involved in the regulation of cell wall expansion and loosening by inducing the expression of *EXP*, *XTH*, and *PECTATE LYASE* (*PL*) genes (Perrot-Rechenmann, 2010; Majda and Robert,

2018), which are necessary for bud break. We discovered that *EXP*, *XTH*, *PL*, and *BGLU* genes are heavily marked by H3K4me3 and are highly expressed at the BB stage (Figure 3d). Several *BGLU* members also modify cell wall integrity (Sampedro *et al*., 2017) and are thought to be marker genes for dormancy release in tree peony (*Paeonia suffruticosa*) (Gao *et al*., 2021). Taken together, H3K4me3 regulates bud break by activating cell cycle regulatory genes and cell wall loosening genes directly or indirectly by enhancing the auxin and GA signaling pathways (Figure 6; right part). Collectively, growth-promoting pathways activating cell metabolism and the cell cycle are possible central targets for epigenetic control that acts in inducing apple bud break in spring.

Finally, we also propose that the increased sensitivity to auxin signaling in spring is conditioned during winter through prolonged chilling–induced H3K4me3 modifications, explaining how cold-mediated epigenetic changes influence bud break in spring (Figures 5 and 6; right part). In parallel, lower sensitivity to ABA signaling during winter is reinforced during spring through warm temperature–induced H3K4me3 modifications. This study thus uncovers both the causal and reinforcing roles of epigenetic regulation in temperature-regulated dormancy progression and break in apple buds.

EXPERIMENTAL PROCEDURES

Plant materials and growth conditions

One-year-old middle branches bearing flower buds at the terminal position were sampled from apple trees (*Malus* × *domestica* Borkh. 'Fuji') grown at the experimental farm of the Department of Agriculture, Shinshu University (Nagano, Japan; 36′ N and 139′ E) on 11 November 2016. Branches were manually defoliated and transferred to our laboratory at Kyoto University (Kyoto, Japan) under ambient temperatures. The next day (12 November 2016), the basal parts of branches were soaked in 1% (v/v) cut-flower preservation reagent (Misakifarm; Otsu Kagaku, Tokushima, Japan) and incubated at 5°C. The samples were covered with a plastic bag to maintain humidity in

an air-conditioned dark room. The bottom parts of the branches were cut, and the solution was refreshed weekly. The flower buds used for the ChIP experiment were collected before the incubation (BC samples) and after a 60-day exposure to chilling (AC samples). Following the chilling treatment, the branches were exposed to forcing conditions in a growth chamber set to 22°C under a long-day photoperiod (16 h light/8 h dark), with a light intensity of 80 μmol m^{-2} s^{-1} provided by cool-white fluorescent lights. The flower buds were collected 9 days into the forcing treatment (BB samples). Bud break was initially observed at 2 weeks after exposing the branches to forcing conditions, and all branches exhibited terminal bud break at 3 weeks (Figure 1a). By contrast, no bud break was observed in BC samples after 4 weeks in forcing conditions, indicating that the BC samples are in the dormancy phase. The BC, AC, and BB flower bud samples (n = 3) were also analyzed by microscopy to examine flower bud development as previously described (Nishiyama *et al.*, 2021). Briefly, flower bud samples were incubated in a 10% sucrose solution followed by frozen Super Cryoembedding Medium (SCEM) (Leica Microsystems GmbH, Wetzlar, Germany). Frozen samples were sectioned using a CM1520 cryostat (Leica). The sections were stained with 0.5% (w/v) toluidine blue for 5 min, embedded in Super Cryo Mounting Medium (SCMM) (Leica), and observed with a BX60 light microscope (Olympus, Tokyo, Japan).

Validation of antibody specificity

Dot blot assays were performed using a modified histone peptide array (Cat. No. 13001: Active Motif Inc., Carlsbad, CA, USA) following the manufacturer's instructions. Briefly, the peptide array chip was soaked in 5% (w/v) non-fat milk in Tris-buffered saline (TBS) buffer (10 mM Tris-HCl, pH 7.4, and 150 mM NaCl) containing 0.05% (v/v) Tween 20 (TBST) and incubated in an orbital shaker for 2 h at room temperature. The peptide array chip was then incubated with primary antibodies against H3K4me3 (Cat. No. ab8580: Abcam, Cambridge, UK) or H3K27me3 (Cat. No. 07-449: Merck Millipore, Burlington, MA, USA) (1:3,000 dilution), followed by HRP-conjugated anti-mouse secondary antibodies (Cat. No. W402B: Promega, Madison, WI, USA) (1:5,000

dilution). After incubation in enhanced chemiluminescence (ECL) reagent (32016, Thermo Fisher Scientific, Waltham, MA, USA), chemiluminescence was detected with an ImageQuant LAS4000mini instrument (GE Healthcare, Chicago, IL, USA).

Chromatin isolation and ChIP-seq analysis

Chromatin samples were prepared, and the immunoprecipitation was performed according to a modified version of a published method (Gendrel *et al.*, 2005). Three to four flower buds were used for each replicate. The crosslinking was completed as previously described (Saito *et al.*, 2015), with minor modifications. Briefly, each flower bud was cut longitudinally several times with a razor and divided into eight equal parts. Samples were crosslinked in 1% (w/v) formaldehyde under vacuum for 10 min at room temperature and again for 5 min after releasing the vacuum. Then, 0.125 M glycine (pH 2.5) was added and the crosslinking reaction was quenched under vacuum for 5 min. The crosslinked samples were washed in sterilized water for 5 s, flash-frozen in liquid nitrogen, and ground to powder. Chromatin was extracted from powder and fragmented using a sonicator (Sonifier 150, Branson). The immunoprecipitation was performed with 5 μL antibody against total histone H3 (Cat. No. ab1791: Abcam) and 10 μL antibody against H3K4me3 or H3K27me3. All experiments were conducted with two biological replicates. DNA fragments were isolated from immunoprecipitated chromatin samples, amplified by PCR, and used to construct sequencing libraries with the ThruPLEX DNA-seq Kit (Cat. No. R400427: Takara Bio, Kusatsu, Japan). The libraries were sequenced with a HiSeq 2000 system (50-bp single-end reads) (Illumina, San Diego, CA, USA).

ChIP-seq data analysis

All Illumina sequencing experiments were conducted at the Vincent J. Coates Genomics Sequencing Laboratory at UC Berkeley, USA. The raw sequencing reads were processed with custom Python scripts developed in the Comai laboratory and available online (http://comailab.genomecenter.ucdavis.edu/index.php/Barcoded_data_preparation_too

ls). Briefly, reads were split based on the index information and trimmed for quality (average Phred sequence quality > 20 over a 5-bp sliding window) and adapter sequences. A minimum read length of 35 bp was applied for the ChIP-seq reads. Unique clean reads (median length of 50 bp) were aligned to the apple genome (GDDH13_11.1) (Daccord *et al.*, 2017) using Bowtie1 (Langmead, 2010), with up to two mismatches allowed. Raw files were filtered to remove PCR duplicates and reads that aligned to multiple locations. The generated wiggle files were used for visualizing the data with the bamCoverage tool in the DeepTools package (Ramírez *et al.*, 2014). Mapped regions were visualized with fluff tools (version 3.0.3) (Georgiou and Van Heeringen, 2016). The ChIP-seq tag-enriched regions were identified by SICER (version 1.1) (Zang *et al.*, 2009), with the following parameters: window size setting of 200 bp and a gap size of 200 bp for H3K4me3; and a window size setting of 200 bp and a gap size of 600 bp for H3K27me3. Input and H3 reads were used as the background. Additionally, a false discovery rate (FDR) of 0.01 was employed. Peaks called by SICER were annotated with the R package ChIPseeker (Yu *et al.*, 2015). To calculate H3K27me3 density, genes were fitted to a length of 10 kb and then divided into five bins. Scores were used to group genes by unsupervised k-means clustering in the DeepTools package (Ramírez *et al.*, 2014) and plotted as heatmaps, presenting each gene in seven bins (−2 kb, five bins from TSS to TES, and +2 kb) (Figure 1b). The H3K4me3 density was determined for the 2-kb fragments surrounding TSSs using five bins and plotted as TSS-centered heatmaps (Figure 1c).

mRNA-seq analysis

To profile gene expression across stages, total RNA was extracted from BC, AC, and BB samples and subjected to RNA-seq analysis using a MGISEQ-2000 instrument (100-bp, paired-end reads) at MGI Tech Co., Ltd. (Beijing, China). The obtained clean reads were mapped to the apple genome (GDDH13_11.1) (Daccord *et al.*, 2017) with HISAT2 (Pertea *et al.*, 2016). StringTie (Pertea *et al.*, 2016) and DESeq2 R (Love *et al.*, 2014) software were used to estimate transcript abundance and identify differentially expressed genes with an FDR threshold of 0.05 in different samples.

Combined ChIP-seq and RNA-seq data mining

Differential ChIP signals were identified with DiffReps (version 1.55.4) (Shen *et al.*, 2013), using H3K27me3, H3K4me3, H3 (background), and input (background) along with default parameters, FDR < 0.001 and fold-change > 1.5 as the cutoff, and a negative binomial test for statistical analyses. Transcribed regions extending 1 kb in each direction from the TSS and TES were used for H3K27me3, and 2-kb regions surrounding TSS were used for H3K4me3. To compare the modifications and gene expression changes over time, the fold-changes of H3K27me3 and H3K4me3 levels identified with DiffReps in the stage transitions BC to AC and AC to BB were normalized against the data for the AC stage. Then, both the relative histone modification levels and related gene expression (as fragments per kilobase per million [FPKM]+1) were $\log_2$-transformed and z-score normalized (Cheadle *et al.*, 2003) separately, and heatmaps were generated using the R package ComplexHeatmap (Gu *et al.,* 2016) with k-means clustering (Figure 3b). For gene expression, FPKM values below 0.5 were considered to reflect very low expression; a minimum expression cutoff of 0.5 FPKM in all three stage samples was therefore applied to exclude low-expressed genes before further analysis. To examine the potential memory role of H3K4me3 in winter on the regulation of gene expression in spring, the genes with increased or decreased histone modification from BC to AC and unchanged from AC to BB stage were extracted. Then, genes with no changes in gene expression from BC to AC but with changes from AC to BB were selected using fluff tools (Georgiou and Van Heeringen, 2016). To examine the potential reinforcing role of H3K4me3 on gene expression changes, the genes with increased or decreased expression levels from BC to AC but unchanged from AC to BB stage were extracted. Then, those with no changes in methylation levels from BC to AC but with changes from AC to BB were selected.

Motif analysis

The candidate targeting motifs by transcription factors that were enriched in the 2-kb promoter regions of H3K27me3- or H3K4me3-marked genes (clusters 1 and 2 in Figure

1b,c) were identified with HOMER software (version 4.10) (Heinz *et al.*, 2010). The 2-kb promoter regions of entire RefSeq genes were used as the background by running the command findMotifsGenome.pl.

GO enrichment analysis

Significant GO enrichment analysis was performed with the clusterprofiler R package (Yu *et al.*, 2012) and Fisher's exact test. An FDR cutoff of 0.05 was selected as the threshold. The GO enriched results were visualized by Revigo (Supek *et al*., 2011).

Quantification of phytohormone contents in dormant flower buds

Freeze-dried BC, AC, and BB samples were ground to a fine powder using a Multi-Beads shocker (Yasui Kikai Co., Osaka, Japan). ABA was extracted from 10 mg of ground powder in a methanol–formic acid buffer (methanol:water:formic acid = 15:4:1, v/v/v) containing a deuterium-labeled phytohormone internal standard (40 ng d6-ABA). Plant hormone extractions (n = 3 from each stage) were conducted overnight at 4°C in darkness. Supernatants were purified with Oasis HLB columns (Waters Co., Milford, MA, USA) and then evaporated. The dry pellets were resuspended in 1 M formic acid and then added to Oasis MCX columns (Waters). Acid and basic fractions were extracted in 100% methanol and 0.35% NH_3 in 60% (v/v) methanol, respectively. The solvents were evaporated from the samples, and the remaining pellets were resuspended in reconstitution solution (acetonitrile:water:formic acid = 85:15:0.1, v/v/v). ABA contents were determined by liquid chromatography–triple quadrupole mass spectrometry (Waters; liquid chromatography system: Waters 2695, mass spectrometer: Quattro micro™ ARI Waters 2996).

Gene family identification and phylogenetic analysis

A Hidden Markov Model (HMM) file retrieved from Pfam (version 32.0) was employed to identify putative MADS-box proteins in the apple proteome with "hmmsearch" of HMMER (version 3.0) (Eddy, 2011) and an e-value below $1e^{-5}$. Arabidopsis homologs were extracted based on gene annotation. Full-length sequences of target proteins from

Arabidopsis and apple were aligned with default parameters in ClustalW2. The aligned sequences were then used to construct a phylogenetic tree according to the neighbor-joining method (1,000 bootstrap replicates) with MEGA7 (Kumar *et al*., 2016).

ACKNOWLEDGEMENTS

We thank Prof. Kiyoshi Banno (Shinshu University, Japan) for allowing us to collect apple branch samples and Mr. Ryuta Hashimoto (Kyoto University, Japan) for RNA extraction. This research was supported by the Grant-in-Aid for Scientific Research (KAKENHI) from the Japan Society for the Promotion of Science (JSPS), Japan (Grant-in-Aid KAKENHI Nos. 23380017, 26252005, 18H02198, 18H04790, 19H05274, and 21H02186), the National Key R&D Program of China (2019YFD1000603), and the National Natural Science Foundation of China (32102324).

AUTHOR CONTRIBUTIONS

HY conceived the original research plans. HY designed and supervised the experiments with help from ZRL and RT. YT and MM performed the ChIP assay. YO completed the microscopy analyses and plant hormone extractions. MGT performed plant hormone measurements. WXC analyzed the ChIP-seq and RNA-seq data and wrote the article with contributions from all authors. YT and HY supervised the writing of the article.

CONFLICT OF INTERESTS

The authors declare that they have no competing interests in this work.

DATA AVAILABILITY STATEMENT

All relevant data can be found within the manuscript and its supporting materials. The ChIP-Seq and RNA-seq data generated in this study have been uploaded to the National Center for Biotechnology Information Gene Expression Omnibus database

(http://www.ncbi.nlm.nih.gov/geo) under the accession number GSE128041 and GSE171131, respectively.

SUPPORTING INFORMATION

Figure S1. Floral primordium development of buds at the BC, AC, and BB stages.

Figure S2. Signal density for H3K27me3 and H3K4me3 in the input and H3 samples.

Figure S3. Dot blot assay validating the specificity of anti-H3K27me3 and anti-H3K4me3 antibodies.

Figure S4. Identification and profiling of *DAM* and *SVP* genes in the apple genome.

Figure S5. H3K4me3 signal density and GO enrichment analysis of genes in each cluster, related to Figure 3b.

Table S1. Enriched DNA-binding motifs in the 2-kb promoter region of H3K27me3-marked genes (clusters 1 and 2 in Figure 1b).

Table S2. Enriched DNA-binding motifs in the 2-kb promoter region of H3K4me3-marked genes (clusters 1 and 2 in Figure 1c).

Table S3. List of H3K4me3-modified DAM-FLC-SVP target genes (Falavigna et al., 2021).

Table S4. Relative H3K4me3 and H3K27me3 levels and expression levels of *DAM* and *FLC* genes, related to Figure 2a.

Table S5. List of H3K27me3 DMGs of which the expression was negatively correlated to H3K27me3 levels.

Table S6. Enriched GO terms of 3,911 genes heavily marked during the BB stage in cluster 3 of Figure 3a.

Table S7. List of the genes of which the H3K4me3 changes in winter played the causal role in the expression change in spring, or vice versa.

REFERENCES

Aksenova, N.P., Sergeeva, L.I., Konstantinova, T.N., Golyanovskaya, S.A., Kolachevskaya, O.O. & Romanov, G.A. (2013) Regulation of potato tuber dormancy and sprouting. *Russian Journal of Plant Physiology*, **60**, 301–312.

Azeez, A., Zhao, Y.C., Singh, R.K., Yordanov, Y.S., Dash, M., Miskolczi, P. *et al*. (2021). EARLY BUD-BREAK 1 and EARLY BUD-BREAK 3 control resumption of poplar growth after winter dormancy. *Nature Communications,* **12**, 1–12.

Bastow, R., Mylne, J.S., Lister, C., Lippman, Z., Martienssen, R.A. & Dean, C. (2004) Vernalization requires epigenetic silencing of *FLC* by histone methylation. *Nature*, **427**, 164–167.

Beauvieux, R., Wenden, B. & Dirlewanger, E. (2018) Bud dormancy in perennial fruit tree species: a pivotal role for oxidative cues. *Frontiers in Plant Science*, **9**, 657.

Benveniste, D., Sonntag, H. J., Sanguinetti, G. & Sproul, D. (2014) Transcription factor binding predicts histone modifications in human cell lines. *Proceedings of the National Academy of Sciences*, **111**, 13367–13372.

Berger, N. & Dubreucq, B. (2012) Evolution goes GAGA: GAGA binding proteins across kingdoms. *Biochimica et Biophysica Acta (BBA)-Gene Regulatory Mechanisms*, **1819**, 863–868.

Brunner, A.M, Evans, L.M., Hsu, C. & Sheng, X. (2014) Vernalization and the chilling requirement to exit bud dormancy: shared or separate regulation? *Frontiers in Plant Science*, **5**, 732.

Buzas, D.M., Robertson, M., Finnegan, E.J. & Helliwell, C.A. (2011). Transcription-dependence of histone H3 lysine 27 trimethylation at the Arabidopsis polycomb target gene *FLC*. *The Plant Journal*, **65**, 872–881.

Buzas, D.M., Tamada, Y. & Kurata, T. (2012). *FLC*: a hidden polycomb response element shows up in silence. *Plant and Cell Physiology*, **53**, 785–793.

Cai, B., Wang, H., Liu, T., Zhuang W., Wang, Z., Qu, S. *et al.* (2019) Effects of gibberellins A_4 on bud break, antioxidant enzymes' activity and proline content of flower buds in sweet cherry (*Prunus avium*). *Acta Physiologiae Plantarum* **41**, 88.

Cheadle, C., Vawter, M.P., Freed, W.J. & Becker, K.G. (2003) Analysis of microarray data using Z score transformation. *The Journal of Molecular Diagnostics*, **5**, 73–81.

Conde, D., Perales, M., Sreedasyam, A., Tuskan, G.A., Lloret, A., Badenes, M.L. *et al.* (2019) Engineering tree seasonal cycles of growth through chromatin modification. *Frontiers in Plant Science*, **10**, 412.

Considine, M.J. & Considine, J.A. (2016) On the language and physiology of dormancy and quiescence in plants. *Journal of Experimental Botany*, **67**, 3189–3203.

Cooke, J.E., Eriksson, M.E. & Junttila, O. (2012) The dynamic nature of bud dormancy in trees: environmental control and molecular mechanisms. *Plant Cell and Environment*, **35**, 1707–1728.

Daccord, N., Celton, J.M., Linsmith, G., Becker, C., Choisne, N., Schijlen, E. *et al.* (2017) High-quality *de novo* assembly of the apple genome and methylome dynamics of early fruit development. *Nature Genetics*, **49**, 1099.

de la Fuente, L., Conesa, A., Lloret, A., Badenes, M.L. & Ríos G. (2015) Genome-wide changes in histone H3 lysine 27 trimethylation associated with bud dormancy release in peach. *Tree Genetics & Genomes*, **11**, 45.

Dietz, K.J., Vogel, M.O. &Viehhauser, A. (2010) AP2/EREBP transcription factors are part of gene regulatory networks and integrate metabolic, hormonal and environmental signals in stress acclimation and retrograde signalling. *Protoplasma*, **245**, 3–14.

Ding, Z., Li, S., An, X., Liu, X., Qin, H. & Wang, D. (2009) Transgenic expression of *MYB15* confers enhanced sensitivity to abscisic acid and improved drought tolerance in *Arabidopsis thaliana*. *Journal of Genetics and Genomics*, **36**, 17–29.

Eddy, S.R. (2011) Accelerated profile HMM searches. *PLoS Computational Biology*, **7**, e1002195.

Falavigna, V.D.S., Guitton, B., Costes, E. & Andrés, F.I. (2019) I want to (bud) break free: the potential role of *DAM* and *SVP-like* genes in regulating dormancy cycle in temperate fruit trees. *Frontiers in Plant Science*, **9**, 1990.

Falavigna V.D.S., Severing E., Lai X., Estevan J., Farrera I., Hugouvieux V. *et al*. (2021). Unraveling the role of MADS transcription factor complexes in apple tree dormancy. *New Phytologist*, **232**, 2071–2088.

Gao, X., Yuan, Y., Liu, Z., Liu, C., Xin, H., Zhang, Y. *et al*. (2021) Chilling and gibberellin acids hyperinduce β-1,3-glucanases to reopen transport corridor and break endodormancy in tree peony (*Paeonia suffruticosa*). *Plant Physiology and Biochemistry*, **167**, 771–784.

Gendrel, A.V., Lippman, Z,, Martienssen, R. & Colot, V. (2005) Profiling histone modification patterns in plants using genomic tiling microarrays. *Nature Methods*, **2**, 213–218.

Georgiou, G., Van & Heeringen, S.J. (2016) fluff: exploratory analysis and visualization of high-throughput sequencing data. *PeerJ*, **4**, e2209.

Grossman, S. R., Engreitz, J., Ray, J. P., Nguyen, T. H., Hacohen, N. & Lander, E. S. (2018) Positional specificity of different transcription factor classes within enhancers. *Proceedings of the National Academy of Sciences*, **115**, E7222–E7230.

Gu, Z., Eils, R. & Schlesner, M. (2016) Complex heatmaps reveal patterns and correlations in multidimensional genomic data. *Bioinformatics*, **32**, 2847–2849.

Heide, O. & Prestrud, A.K. (2005) Low temperature, but not photoperiod, controls growth cessation and dormancy induction and release in apple and pear. *Tree Physiology*, **25**, 109–114.

Heinz, S., Benner, C., Spann, N., Bertolino, E., Lin, Y., Laslo, P. *et al.* (2010) Simple combinations of lineage-determining transcription factors prime cis-regulatory elements required for macrophage and B cell identities. *Molecular Cell*, **38**, 576–589.

Heo, J. B. & Sung, S. (2011). Vernalization-mediated epigenetic silencing by a long intronic noncoding RNA. *Science*, **331**, 76-79.

Horvath, D. (2009) Common mechanisms regulate flowering and dormancy. *Plant Science*, **177**, 523–531.

Horvath, D.P., Anderson, J.V., Chao, W.S. & Foley, M.E. (2003) Knowing when to grow: signals regulating bud dormancy. *Trends in Plant Science*, **8**, 534–540.

Horvath, D.P., Sung, S., Kim, D., Chao, W. & Anderson, J. (2010) Characterization, expression and function of *DORMANCY ASSOCIATED MADS-BOX* genes from leafy spurge. *Plant Molecular Biology*, **73,** 169–179.

Hsiang, T.F., Chen, W. & Yamane, H. (2021) The *MADS-Box* gene family involved in the regulatory mechanism of dormancy and flowering in Rosaceae fruit trees. *Annual Plant Reviews Online*, **4**, 649–686.

Ishikawa, M., Morishita, M., Higuchi, Y., Ichikawa, S., Ishikawa, T., Nishiyama, T. *et al.* (2019) Physcomitrella STEMIN transcription factor induces stem cell formation with epigenetic reprogramming. *Nature Plants*, **5**, 681–690.

Kumar, S., Stecher, G. & Tamura, K. (2016) MEGA7: molecular evolutionary genetics analysis version 7.0 for bigger datasets. *Molecular Biology and Evolution*, **33**, 1870–1874.

Lang, G.A., Early, J.D., Martin, G.C. & Darnell, R.L. (1987) Endo-, para-, and ecodormancy: physiological terminology and classification for dormancy research. *HortScience*, **22,** 371–377.

Langmead, B. (2010) Aligning short sequencing reads with Bowtie. *Current Protocols in Bioinformatics*, **32**, 11–7.

Leida, C., Conesa, A., Llácer, G., Badenes, M.L. & Ríos, G. (2012) Histone modifications and expression of *DAM6* gene in peach are modulated during bud dormancy release in a cultivar-dependent manner. *New Phytologist*, **193**, 67–80.

Li, Z., Li, B., Liu, J., Guo, Z., Liu, Y., Li, Y. *et al.* (2016) Transcription factors AS1 and AS2 interact with LHP1 to repress *KNOX* genes in Arabidopsis. *Journal of Integrative Plant Biology*, **58**, 959–970.

Liu, J. & Sherif, S.M. (2019) Hormonal orchestration of bud dormancy cycle in deciduous woody perennials. *Frontiers in Plant Science*, **10**, 1136.

Love, M.I., Huber, W. & Anders, S. (2014) Moderated estimation of fold change and dispersion for RNA-seq data with DESeq2. *Genome Biology*, **15**, 550.

Majda, M. & Robert, S. (2018) The role of auxin in cell wall expansion. *International Journal of Molecular Sciences*, **19**, 951.

Michaels, S.D. & Amasino, R.M. (1999) *FLOWERING LOCUS C* encodes a novel

MADS domain protein that acts as a repressor of flowering. *The Plant Cell*, **11**, 949–956.

Ng, D.W.K. & Hall, T.C. (2008) PvALF and FUS3 activate expression from the phaseolin promoter by different mechanisms. *Plant Molecular Biology,* **66**, 233–244.

Nishiyama, S., Matsushita, M.C., Yamane, H., Honda, C., Okada, K., Tamada, Y. *et al.* (2021) Functional and expressional analyses of apple *FLC*-like in relation to dormancy progress and flower bud development. *Tree Physiology*, **41**, 562–570.

Or, E., Vilozny, I., Eyal, Y. & Ogrodovitch, A. (2000). The transduction of the signal for grape bud dormancy breaking induced by hydrogen cyanamide may involve the SNF-like protein kinase GDBRPK. *Plant Molecular Biology*, **43**, 483-494.

Perrot-Rechenmann, C. (2010) Cellular responses to auxin: division versus expansion. *Cold Spring Harbor Perspectives in Biology*, **2**, a001446.

Pertea, M., Kim, D., Pertea, G.M., Leek, J.T. & Salzberg, S.L. (2016) Transcript-level expression analysis of RNA-seq experiments with HISAT, StringTie and Ballgown. *Nature Protocols*, **11**, 1650.

Porto, D.D., Bruneau, M., Perini, P., Anzanello, R., Renou, J.P., Santos, H.P.d. *et al.* (2015) Transcription profiling of the chilling requirement for bud break in apples: a putative role for *FLC-like* genes. *Journal of Experimental Botany*, **66**, 2659–2672.

Ramírez, F., Dündar, F., Diehl, S., Grüning, B.A. & Manke, T. (2014) deepTools: a flexible platform for exploring deep-sequencing data. *Nucleic Acids Research*, **42**, W187–W191.

Rinne, PL., Welling, A., Vahala, J., Ripel, L., Ruonala, R., Kangasjärvi, J. *et al.* (2011) Chilling of dormant buds hyperinduces *FLOWERING LOCUS T* and recruits GA-inducible 1,3-β-glucanases to reopen signal conduits and release dormancy in *Populus*. *Plant Cell*, **23**, 130–146.

Ríos, G., Leida, C., Conejero, A. & Badenes, M.L. (2014) Epigenetic regulation of bud dormancy events in perennial plants. *Frontiers in Plant Science*, **5**, 247.

Saito, T., Bai, S., Imai, T., Ito, A., Nakajima, I. & Moriguchi, T. (2015) Histone

modification and signalling cascade of the *dormancy-associated MADS-box* gene, *PpMADS 13-1*, in Japanese pear (*Pyrus pyrifolia*) during endodormancy. *Plant Cell and Environment*, **38**, 1157–1166.

Saito, T., Wang, S., Ohkawa, K., Ohara, H., Ikeura, H., Ogawa, Y. *et al.* (2017) Lipid droplet-associated gene expression and chromatin remodelling in LIPASE 5′-upstream region from beginning- to mid- endodormant bud in 'Fuji' apple. *Plant Molecular Biology*, **95**, 441–449.

Sampedro, J., Valdivia, E.R., Fraga, P., Iglesias, N., Revilla, G. & Zarra, I. (2017) Soluble and membrane-bound β-glucosidases are involved in trimming the xyloglucan backbone. *Plant Physiology*, **173**, 1017–1030.

Sasaki, R., Yamane, H., Ooka, T., Jotatsu, H., Kitamura, Y., Akagi, T. *et al.* (2011). Functional and expressional analyses of *PmDAM* genes associated with endodormancy in Japanese apricot. *Plant Physiology*, **157**, 485–497.

Shen, L., Shao, N., Liu, X., Maze, I., Feng, J. & Nestler, E,J. (2013) diffReps: detecting differential chromatin modification sites from ChIP-seq data with biological replicates. *PLoS One*, **8**, e65598.

Shimizu-Sato, S. & Mori, H. (2001) Control of outgrowth and dormancy in axillary buds. *Plant Physiology*, **127**, 1405–1413.

Stortenbeker, N. & Bemer, M. (2019). The *SAUR* gene family: the plant's toolbox for adaptation of growth and development. *Journal of Experimental Botany*, **70**, 17–27.

Sung, S. & Amasino, R.M. (2004). Vernalization in Arabidopsis thaliana is mediated by the PHD finger protein VIN3. *Nature*, **427**, 159–164.

Supek, F., Bošnjak, M., Škunca, N. & Šmuc, T. (2011) REVIGO summarizes and visualizes long lists of gene ontology terms. *PLoS One*, **6**, e21800.

Swiezewski, S., Liu, F., Magusin, A. & Dean, C. (2009). Cold-induced silencing by long antisense transcripts of an *Arabidopsis* Polycomb target. *Nature*, **462**, 799–802.

Takeuchi, T., Matsushita, M.C., Nishiyama, S., Yamane, H., Banno, K. & Tao, R. (2018) RNA-sequencing analysis identifies genes associated with chilling-

mediated endodormancy release in apple. *Journal of the American Society for Horticultural Science*, **143**, 194–206.

Tamada, Y., Yun, J.Y., Woo, S.C. & Amasino, R.M. (2009). *ARABIDOPSIS TRITHORAX-RELATED7* is required for methylation of lysine 4 of histone H3 and for transcriptional activation of *FLOWERING LOCUS C*. *The Plant Cell*, **21**, 3257–3269.

Tuan, P.A., Bai, S., Saito, T., Imai, T., Ito, A. & Moriguchi, T. (2016) Involvement of *EARLY BUD-BREAK*, an AP2/ERF transcription factor gene, in bud break in Japanese pear (*Pyrus pyrifolia* Nakai) lateral flower buds: expression, histone modifications and possible target genes. *Plant and Cell Physiology*, **57**, 1038–1047.

Tuan, P.A., Bai, S., Saito, T., Ito, A. & Moriguchi, T. (2017) *Dormancy-associated MADS-Box* (*DAM*) and the abscisic acid pathway regulate pear endodormancy through a feedback mechanism. *Plant and Cell Physiology*, **58**, 1378–1390.

Tylewicz, S., Petterle, A., Marttila, S., Miskolczi, P., Azeez, A., Singh, R.K. *et al.* (2018) Photoperiodic control of seasonal growth is mediated by ABA acting on cell-cell communication. *Science*, **360**, 212–215.

Vimont, N., Quah, F.X., Schöepfer, D.G., Roudier, F., Dirlewanger, E., Wigge, P.A. *et al.* (2020) ChIP-seq and RNA-seq for complex and low-abundance tree buds reveal chromatin and expression co-dynamics during sweet cherry bud dormancy. *Tree Genetics & Genomes*, **16**, 9.

Vimont, N., Schwarzenberg, A., Domijan, M., Beauvieux, R., Arkoun, M., Yvin, J. *et al.* (2021) Fine tuning of hormonal signaling is linked to dormancy status in sweet cherry flower buds. *Tree Physiology*, **41,** 544–561.

Voogd, C., Brian, L.A., Wu, R., Wang, T., Allan, A.C. & Varkonyi-Gasic, E. (2021). A MADS-box gene with similarity to *FLC* is induced by cold and correlated with epigenetic changes to control budbreak in kiwifruit. *New Phytologist*, https://doi.org/10.1111/nph.17916.

Xu, G., Tao, Z. & He, Y. (2022) Embryonic reactivation of *FLOWERING LOCUS C* by ABSCISIC ACID-INSENSITIVE 3 establishes the vernalization requirement

in each Arabidopsis generation. https://doi.org/10.1093/plcell/koac077

Wu, R., Cooney, J., Tomes, S., Rebstock, R., Karunairetnam, S., Allan, A.C. *et al.* (2021) RNAi-mediated repression of dormancy-related genes results in evergrowing apple trees. *Tree Physiology*, tpab007.

Xiao, J., Lee, U.S. & Wagner, D. (2016) Tug of war: adding and removing histone lysine methylation in *Arabidopsis*. *Current Opinion in Plant Biology*, **34**, 41-53.

Xu, C., Luo, F. & Hochholdinger, F. (2016) LOB domain proteins: beyond lateral organ boundaries. *Trends in Plant Science*, **21**, 159–167.

Yamane, H., Wada, M., Honda, C., Matsuura, T., Ikeda, Y., Hirayama, T. *et al.* (2019) Overexpression of Prunus *DAM6* inhibits growth, represses bud break competency of dormant buds and delays bud outgrowth in apple plants. *PLoS One*, **14**, e0214788.

Yang, Q., Gao, Y., Wu, X., Moriguchi, T., Bai, S. & Teng, Y. (2021) Bud endodormancy in deciduous fruit trees: advances and prospects. *Horticulture Research*, **8**, 1–11.

Yang, Q., Niu, Q., Li, J., Zheng, X., Ma, Y., Bai, S. *et al.* (2018) PpHB22, a member of HD-Zip proteins, activates *PpDAM1* to regulate bud dormancy transition in 'Suli' pear (*Pyrus pyrifolia* White Pear Group) *Plant Physiology and Biochemistry*, **127**, 355–365.

Yang, Q., Yang, B., Li, J., Wang, Y., Tao, R., Yang, F. *et al.* (2020) ABA-responsive ABRE-BINDING FACTOR3 activates *DAM3* expression to promote bud dormancy in Asian pear. *Plant, Cell & Environment*, **43**, 1360–1375.

Yu, G., Wang, L., Han, Y. & He, Q. (2012) clusterProfiler: an R package for comparing biological themes among gene clusters. *OMICS: A Journal of Integrative Biology*, **16**, 284–287.

Yu, G., Wang, L. & He, Q. (2015) ChIPseeker: an R/Bioconductor package for ChIP peak annotation, comparison and visualization. *Bioinformatics*, **31**, 2382–2383.

Zang, C., Schones, D., Zeng, C., Cui, K., Zhao, K. & Peng, W. (2009) A clustering approach for identification of enriched domains from histone modification ChIP-Seq data. *Bioinformatics*, **25**, 1952–1958.

Zhang, X., Bernatavichute, Y.V., Cokus, S., Pellegrini, M. & Jacobsen, S.E. (2009) Genome-wide analysis of mono-, di- and trimethylation of histone H3 lysine 4 in *Arabidopsis thaliana*. *Genome Biology*, **10**, R62.

Zhang, X., Clarenz, O., Cokus, S., Bernatavichute, Y.V., Pellegrini, M., Goodrich, J. *et al.* (2007) Whole-genome analysis of histone H3 lysine 27 trimethylation in *Arabidopsis*. *PLoS Biology*, **5**, e129.

Zhang, Z., Shi, L., Dawany, N., Kelsen, J., Petri, M.A. & Sullivan, K.E. (2016) H3K4 tri-methylation breadth at transcription start sites impacts the transcriptome of systemic lupus erythematosus. *Clinical Epigenetics*, **8**, 14.

Zhang, Z., Zhuo, X., Zhao, K., Zheng, T., Han, Y., Yuan, C. & Zhang, Q. (2018) Transcriptome profiles reveal the crucial roles of hormone and sugar in the bud dormancy of *Prunus mume*. *Scientific Reports*, **8**, 1–15.

Zhao Y., Christensen, S.K., Fankhauser, C., Cashman, J.R., Cohen, J.D., Weigel, D. *et al.* (2001) A role for flavin monooxygenase-like enzymes in auxin biosynthesis. *Science*, **291**, 306–309.

Zheng, C., Kwame Acheampong, A., Shi, Z., Halaly, T., Kamiya, Y., Ophir, R. *et al*. (2018) Distinct gibberellin functions during and after grapevine bud dormancy release. *Journal of Experimental Botany*, **69**, 1635–1648.

Zhu, H., Chen, P., Zhong, S., Dardick, C., Callahan, A., An, Y.Q. *et al*. (2020) Thermal-responsive genetic and epigenetic regulation of *DAM* cluster controlling dormancy and chilling requirement in peach floral buds. *Horticulture Research*, **7**, 1–14.

Zhuang, W., Gao, Z., Wang, L., Zhong, W., Ni, Z. & Zhang, Z. (2013) Comparative proteomic and transcriptomic approaches to address the active role of GA_4 in Japanese apricot flower bud dormancy release. *Journal of Experimental Botany*, **64**, 4953–4966.

Zong, X., Zhang, Y., Walworth, A., Tomaszewski, E. M., Callow, P., Zhong, G.Y. *et al*. (2019). Constitutive expression of an apple *FLC3-like* gene promotes flowering in transgenic blueberry under nonchilling conditions. *International Journal of Molecular Sciences*, **20**, 2775.

FIGURE LEGENDS

Figure 1. Global view of H3K27me3- and H3K4me3-occupied sites across bud dormancy phases. (**a**) Sampling conditions and representative images of the buds used for the ChIP-seq and RNA-seq analyses. Dormant terminal flower buds (before chilling, BC samples) were exposed to chilling (5°C, darkness) for 60 days (after chilling, AC samples). The buds were then exposed to forcing conditions (22°C, 16-h-light/8-h-dark photoperiod) for 9 days just before bud break (bud break stage, BB samples). (**b**) K-means clustering (k = 5) of the H3K27me3 enrichment at all RefSeq genes across samples. For H3K27me3, gene bodies 2 kb upstream of the transcription start site (TSS) and 2 kb downstream of the transcription end site (TES) were used for analysis. Genes are arrayed according to their signal score (per bp of marked length). (**c**) K-means clustering (k = 5) of the H3K4me3 enrichment at all RefSeq genes across samples. For H3K4me3, the region ± 2 kb of the TSS was examined. Genes are arrayed according to their signal score (per bp of marked length). (**d**) Boxplot of gene expression levels in each cluster according to their H3K27me3 (upper) and H3K4me3 (bottom) levels in the BC (left), AC (middle), and BB (right) stages. The box extends from the 25^{th} to 75^{th} percentiles, the horizontal line in the box indicates the median, and the whiskers are drawn down to the 10^{th} and up to the 90^{th} percentile. The outliers below and above the whiskers are drawn as individual points. The one-way ANOVA followed by Tukey HSD test was used to test statistical significance. Lower case letters indicate significant differences ($P < 0.05$) in relative expression levels between the clusters.

Figure 2. Histone methylation and expression levels of MADS-box genes and abscisic acid (ABA) contents during bud dormancy progression. (**a**) Distribution of H3K27me3, H3K4me3, and RNA-seq reads at representative *DAM* and *FLC* loci. Y-axis indicates the normalized read number to total read number (per million reads) illustrated with

fluff tools. (**b**) ABA contents in dormant flower buds in BC, AC, and BB stages. Significant differences are indicated by a and b, examined by Tukey's multiple comparison test ($P < 0.05$).

Figure 3. Dynamic changes to H3K4me3 drive seasonal gene expression. (**a**) Frequency distribution of Pearson's rank correlation coefficients between the stage dynamics of mRNA and H3K27me3 (left) and H3K4me3 (right). (**b**) Relative H3K4me3 and expression levels of H3K4me3 DMGs of which the expression was positively correlated with the H3K4me3 levels throughout stages or in transition from BC to AC or AC to BB (left). The color key and number under the heatmap represent the relative levels (z-scores). Clustering analysis was performed according to H3K4me3 levels across stages. Gene Ontology (GO) terms related to biological process enriched in cluster 3 (right) were extracted and shown using Revigo analysis. Related terms are visualized with the same colors. Size of the rectangles represent the *P* value of the GO terms. (**c**) Distribution of H3K4me3 and RNA-seq reads at representative loci of each cluster. Gene ID, *SnRK2.7*, *CXXS1*, *CYCD3-2*, *GLIP*. Y-axis indicates the normalized read number to total read number (per million reads) illustrated with fluff tools. (**d**) Relative H3K4me3 and expression levels of genes related to cell cycle and cell wall modification. The fractions in parentheses indicate the total number of gene members (denominator) and the number of DEG members (numerator).

Figure 4. H3K4me3 and expression profiles of hormone-related genes across dormancy stages. (**a**) Relative H3K4me3 and expression levels of auxin and gibberellin (GA)-related genes. The fractions in parentheses indicate the total number of gene members (denominator) and the number of differential gene members (numerator). (**b**) Distribution of H3K4me3 and RNA-seq reads at auxin- and GA-related genes. Y-axis indicates the normalized read number to total read number (per million reads) illustrated with fluff tools.

Figure 5. Prolonged chilling–induced H3K4me3 and gene expression changes in winter,

respectively, preceded gene expression and H3K4me3 change during bud break in spring. (**a**) Relative H3K4me3 and expression levels of genes at which H3K4me3 levels increase (histone go up earlier) or decrease (histone go down earlier) in the AC stage followed by the change of transcript levels in BB stage or the genes that show decreased expression levels earlier in AC stage followed by decreased H3K4me3 levels later in the BB stage (gene go down earlier). (**b**) H3K4me3 density (upper) and gene expression level (bottom) of genes in each cluster. (**c**) Distribution of histone mark and RNA-seq reads at representative loci for each cluster. Y-axis indicates the normalized read number to total read number (per million reads) illustrated with fluff tools.

Figure 6. Hypothetical model illustrating the epigenetic regulations during apple bud dormancy progression and break. Hypothetical epigenetic regulations and gene regulatory network involving epigenetic regulations in late autumn (left part), winter (center part), and spring (right part) were drawn.

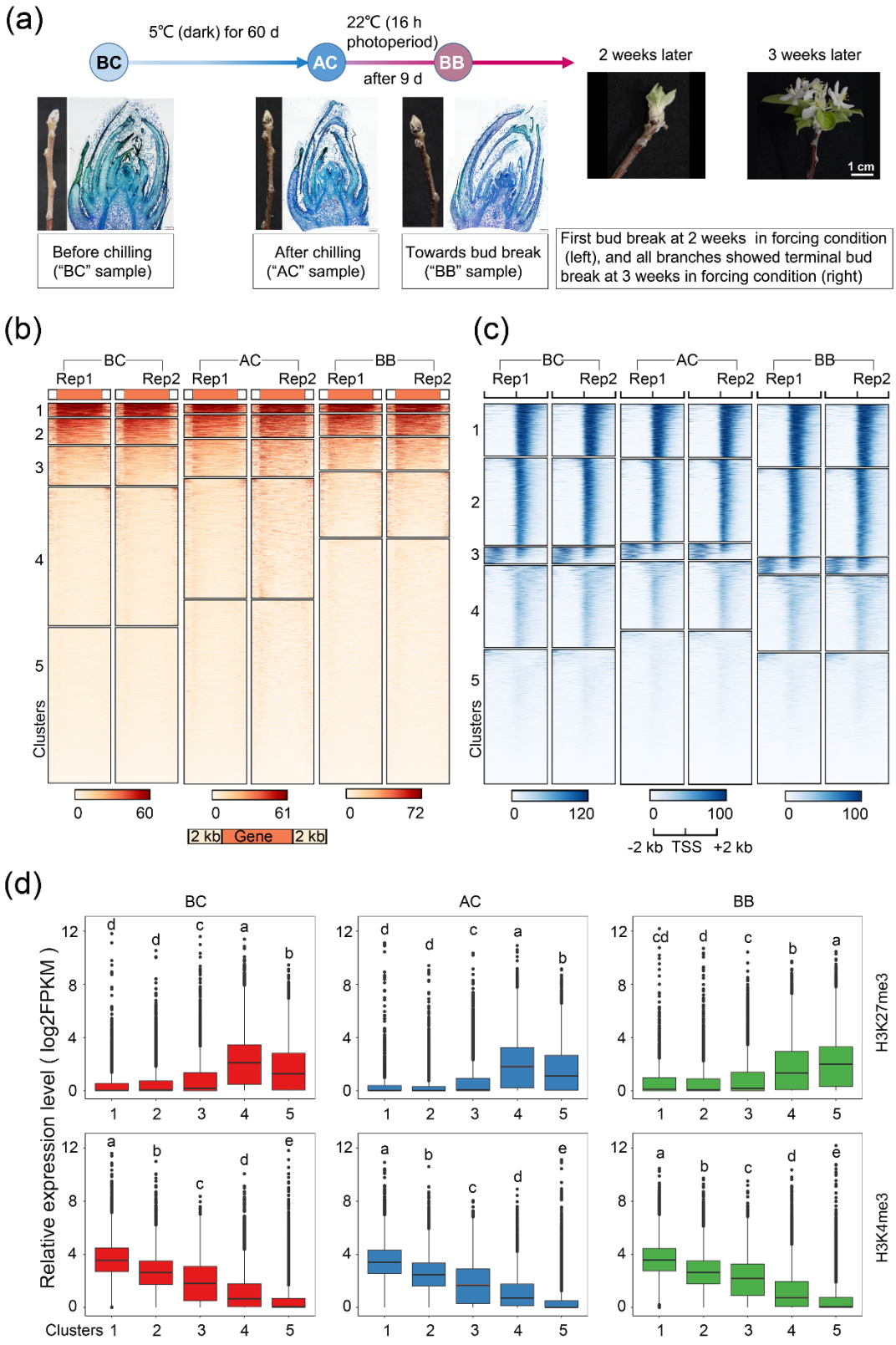

Figure 1. Global view of H3K27me3- and H3K4me3-occupied sites across bud dormancy phases. (**a**) Sampling conditions and representative images of the buds used for the ChIP-seq and RNA-seq analyses. Dormant terminal flower buds (before chilling,

BC samples) were exposed to chilling (5°C, darkness) for 60 days (after chilling, AC samples). The buds were then exposed to forcing conditions (22°C, 16-h light / 8-h dark photoperiod) for nine days just before bud break (bud break stage, BB samples). (**b**) K-means clustering (k = 5) of the H3K27me3 enrichment at all RefSeq genes across samples. For H3K27me3, gene bodies, 2 kb upstream of the transcription start site (TSS), and 2 kb downstream of the transcription end site (TES) were used for analysis. Genes are arrayed according to their signal score (per bp of marked length). (**c**) K-means clustering (k = 5) of the H3K4me3 enrichment at all RefSeq genes across samples. For H3K4me3, the region ± 2 kb of the TSS was examined. Genes are arrayed according to their signal score (per bp of marked length). (**d**) Boxplot of gene expression levels in each cluster according to their H3K27me3 (upper) and H3K4me3 (bottom) levels in the BC (left), AC (middle), and BB (right) stages. The box extends from the 25th to 75th percentiles, the horizontal line in the box indicates the median, and the whiskers are drawn down to the 10th and up to the 90th percentile. The outliers below and above the whiskers are drawn as individual points. The one-way ANOVA followed by Tukey HSD test was used to test statistical significance. Lower case letters indicate significant differences ($P < 0.05$) in relative expression levels between the clusters.

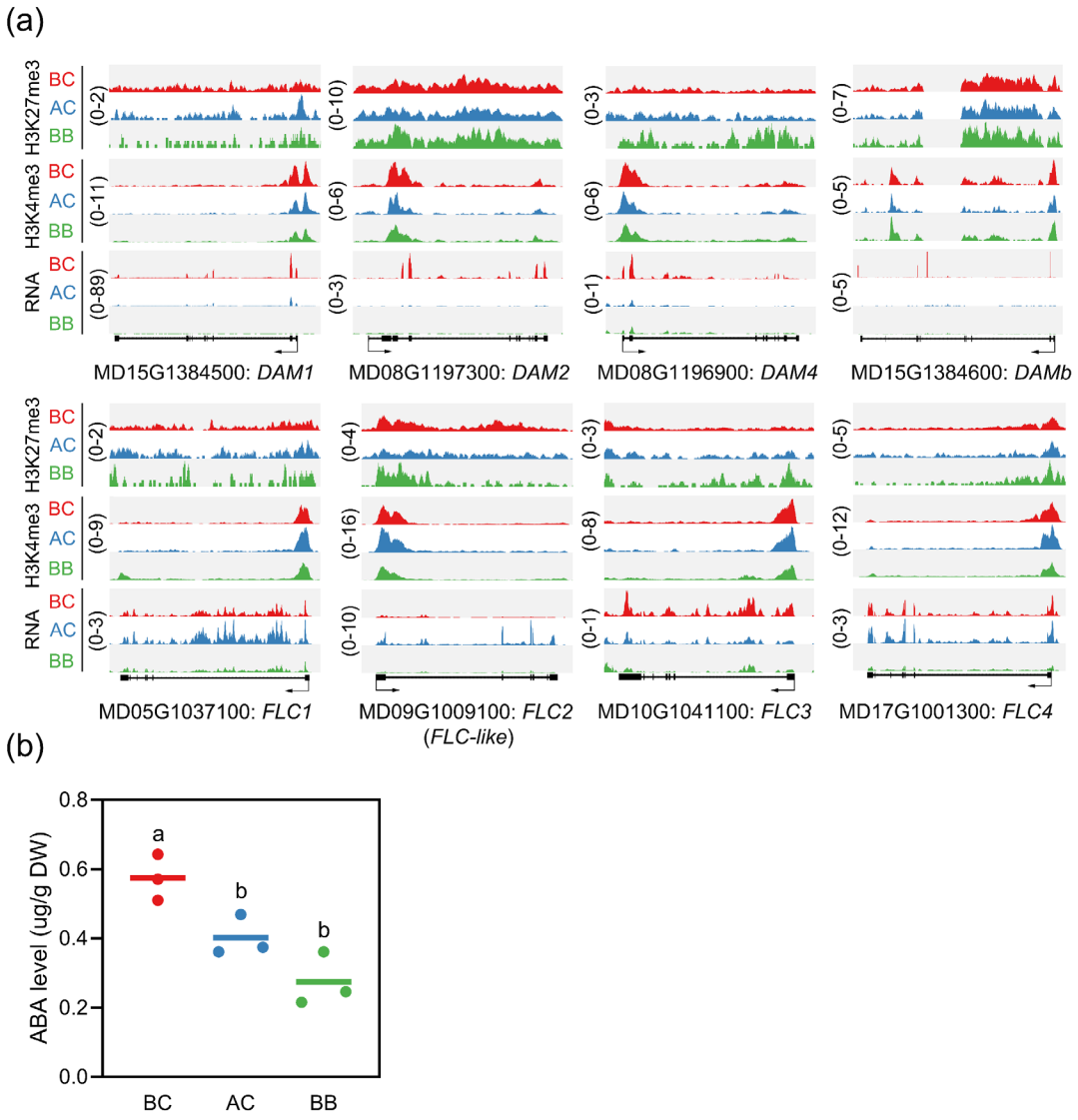

Figure 2. Histone methylation and expression levels of MADS-box genes and abscisic acid (ABA) contents during bud dormancy progression (**a**) Distribution of H3K27me3, H3K4me3, and RNA-seq reads at representative *DAM* and *FLC* loci. Y-axis indicates the normalized read number to total read number (per million reads) illustrated with fluff tools. (**b**) ABA contents in dormant flower buds in BC, AC, and BB stages. Significant differences are indicated by a and b, examined by Tukey's multiple comparison test ($P < 0.05$).

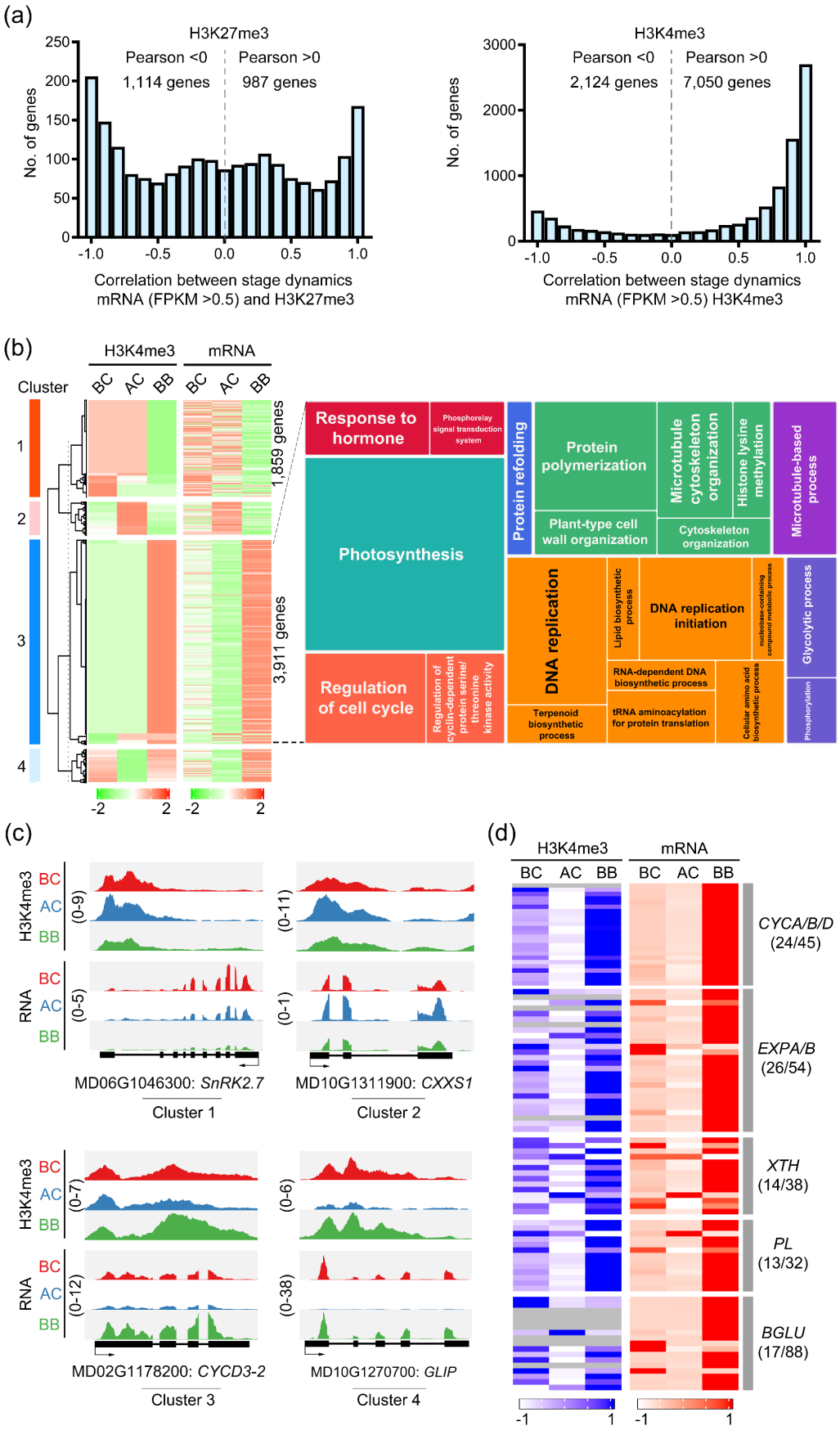

Figure 3. Dynamic changes to H3K4me3 drive seasonal gene expression. (**a**)

Frequency distribution of Pearson's rank correlation coefficients between the stage dynamics of mRNA and H3K27me3 (left) and H3K4me3 (right). (**b**) Relative H3K4me3 and expression levels of H3K4me3 DMGs of which the expression was positively correlated with the H3K4me3 levels throughout stages or in either transition from BC to AC or AC to BB (left). The color key and number under the heatmap represents the relative levels (z-scores). Clustering analysis was performed according to H3K4me3 levels across stages. Gene Ontology (GO) terms related to biological process enriched in cluster 3 (right) were extracted and shown by using Revigo analysis. Related terms are visualized with same colors. Size of the rectangles represent the *p*-value of the GO terms. (**c**) Distribution of H3K4me3 and RNA-seq reads at representative loci of each cluster. Gene ID, *SnRK2.7*, *CXXS1*, *CYCD3-2*, *GLIP*. Y-axis indicates the normalized read number to total read number (per million reads) illustrated with fluff tools. (**d**) Relative H3K4me3 and expression levels of genes related to cell cycle and cell wall modification. The fractions in parentheses indicate the total number of gene members (denominator) and the number of DEG members (numerator).

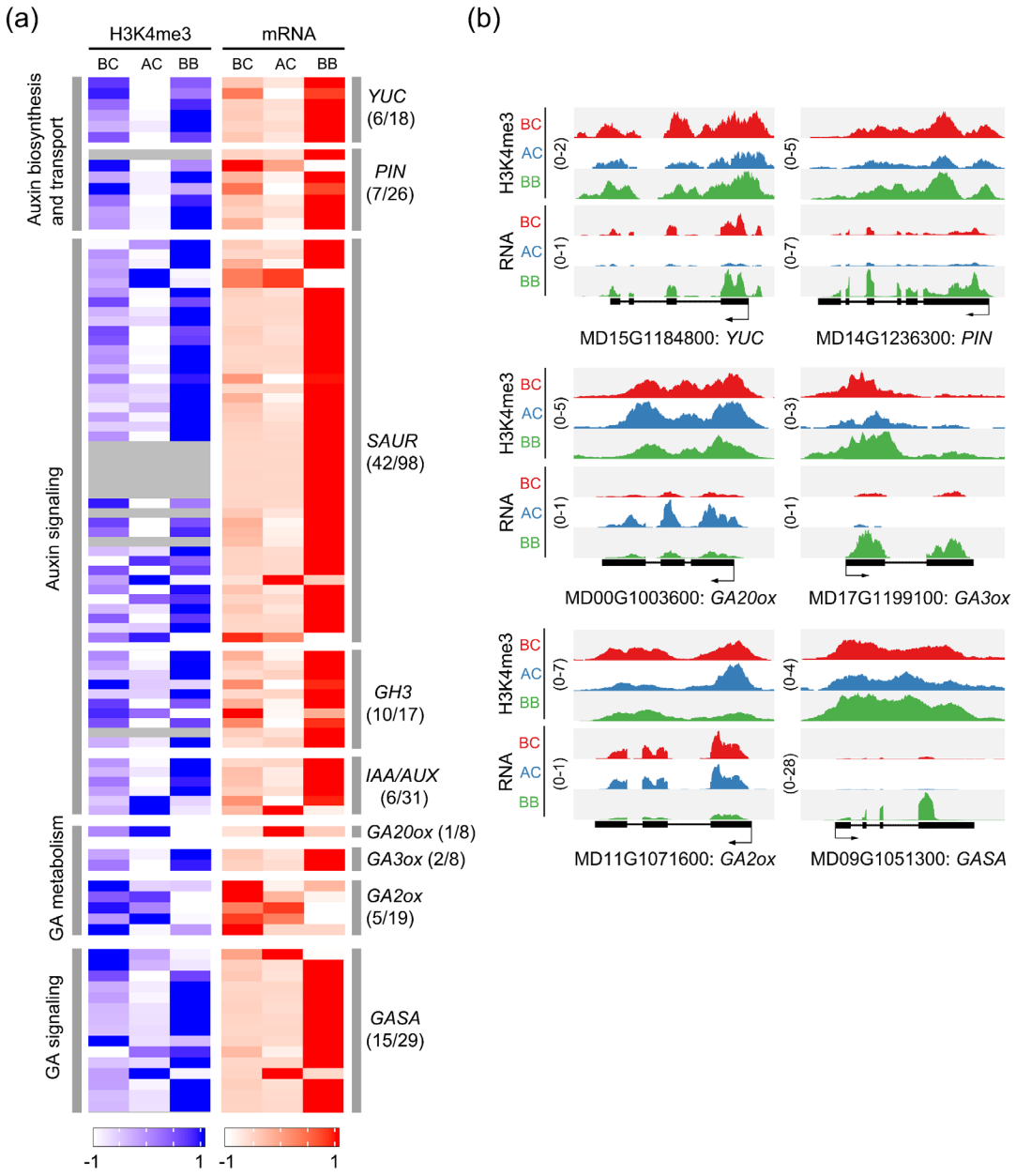

Figure 4. H3K4me3 and expression profiles of hormone-related genes across dormancy stages. (**a**) Relative H3K4me3 and expression levels of auxin and gibberellin (GA)-related gene. The fractions in parentheses indicate the total number of gene members (denominator) and the number of differential gene members (numerator). (**b**) Distribution of H3K4me3 and RNA-seq reads at auxin and GA-related genes. Y-axis indicates the normalized read number to total read number (per million reads) illustrated with fluff tools.

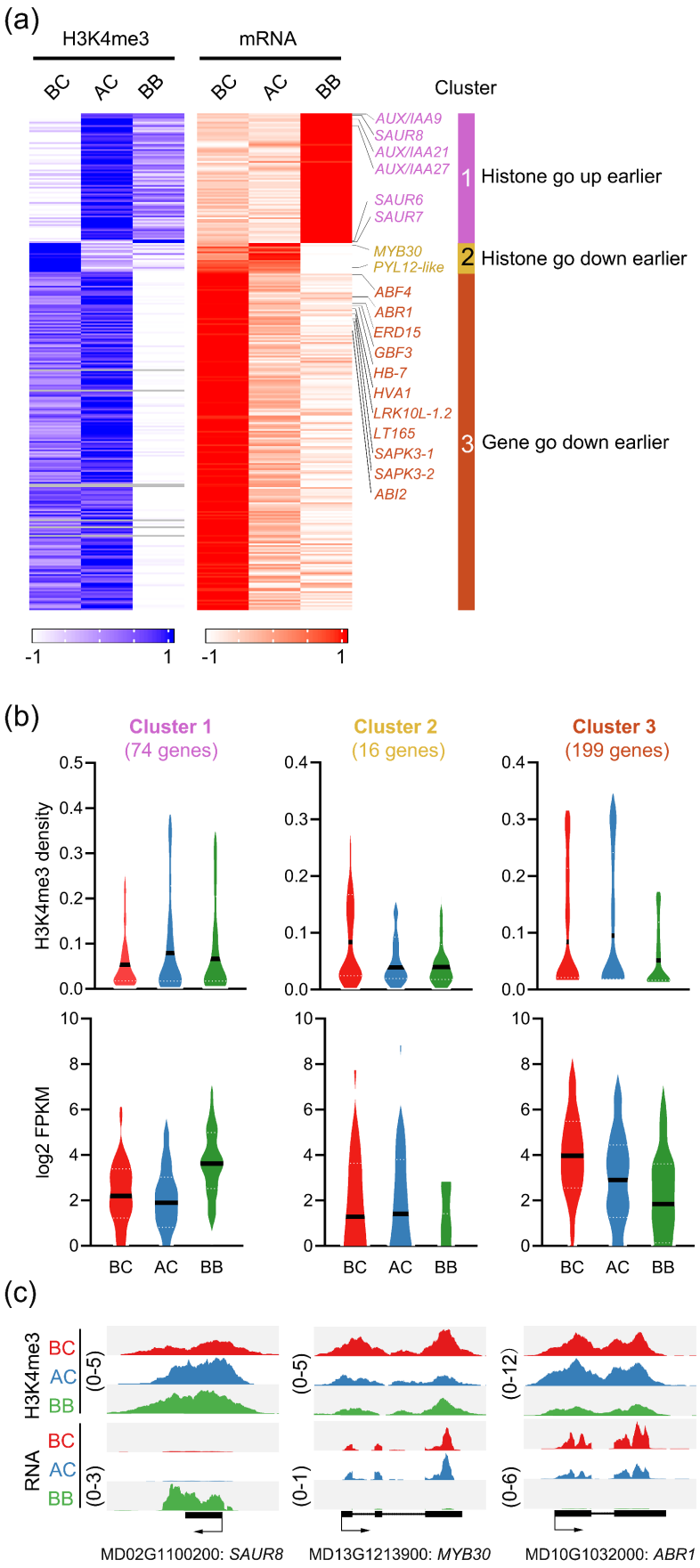

Figure 5. Prolonged chilling-induced H3K4me3 and gene expression change in winter,

respectively, preceded gene expression and H3K4me3 change during bud break in spring. (**a**) Relative H3K4me3 and expression levels of genes at which H3K4me3 levels increase (histone go up earlier) or decrease (histone go down earlier) in AC stage followed by the change of transcript levels in BB stage, or the genes that show decreased expression levels earlier in AC stage followed by decreased H3K4me3 levels later in BB stage (gene go down earlier). (**b**) H3K4me3 density (upper) and gene expression level (bottom) of gene in each cluster. (**c**) Distribution of histone mark and RNA-seq reads at representative loci for each cluster. Y-axis indicates the normalized read number to total read number (per million reads) illustrated with fluff tools.

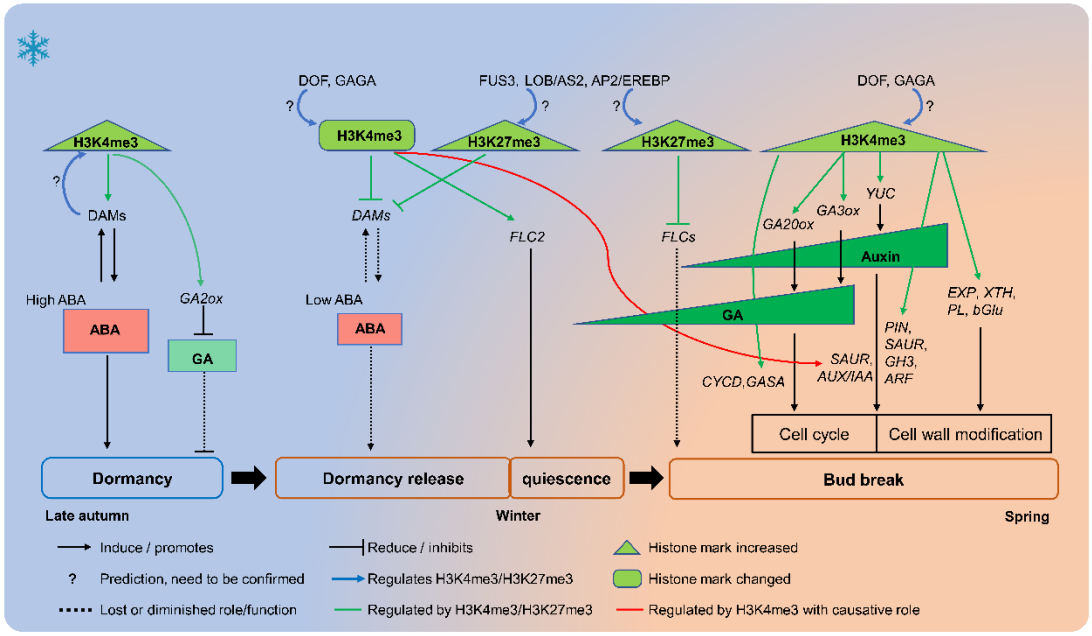

Figure 6. Hypothetical model illustrating the epigenetic regulations during apple bud dormancy progression and break. Hypothetical epigenetic regulations and gene regulatory network involving epigenetic regulations in late autumn (left part), winter (center part), and spring (right part) were drawn.